Joint Interference Cancellation with Imperfect CSI

Zhibin Zou*[†], Xue Wei*[†], Xin Tian*, Genshe Chen*, Aveek Dutta[†], Khanh Pham[‡] and Erik Blasch[‡]

* Intelligent Fusion Technology, Inc., Germantown, MD 20874, USA

† Department of Electrical and Computer Engineering, University at Albany, SUNY, NY 12222, USA

[‡]Air Force Research Laboratory, Arlington, VA 22203, USA

Email: †{zzou2, xwei4, adutta}@albany.edu, *{xtian, gchen}@intfusiontech.com, ‡{khanh.pham.1, erik.blasch.1}@us.af.mil

Abstract-Precoding and Modulation techniques are widely investigated to mitigate interference in the space, time, and frequency domains, respectively. However, next-generation (xG) channels are increasingly dense and mobile, making these domains highly correlated and resulting in high-dimensional channel tensors. Separate interference cancellation methods treating the channel as independent 2-D matrices fail to cancel the joint interference across multiple Degrees of Freedom (DoF). High Order Generalized Mercer's Theorem (HOGMT) based precoding and Multidimensional Eigenwave Multiplexing (MEM) modulation have been proposed to cancel the joint interference by leveraging the jointly orthogonal eigencomponents of the channel. However, these methods rely heavily on perfect Channel State Information (CSI), and their performance degrades with imperfect CSI. In this paper, we propose a joint interference cancellation method based on the Convolutional Neural Network (CNN) with a single linear kernel (JIC-CLK). We show that a CNN with a single linear kernel is equivalent to a wireless system, where the linear kernel itself is identical to the transmitted signal with the CSI as input. By training the output to approach the desired signal at the receiver with MSE loss, the kernel converges to the optimal transmitted signal in the MMSE sense. The proposed method adapts to both perfect and imperfect CSI and can be extended to high-dimensional channels. The accuracy and generality of the proposed method are validated by simulations in three cases: 1) Perfect CSI, 2) Imperfect CSI, and 3) 4-D spatio-temporal channels with imperfect CSI.

Keywords—Convolutional Neural Network, Interference Cancellation, Imperfect CSI, Multi-dimensional Channels.

I. INTRODUCTION

In general, precoding is employed for spatial interference cancellation in MU-MIMO channels. It requires CSI to capture the mutual effects among users and then design the precoding matrix to cancel Inter-User Interference (IUI). Conventional linear precoding methods include Maximum Ratio Transmission (MRT), Zero-Forcing (ZF), and MMSE Precoding. MRT maximizes the signal power at the intended user and is suitable for systems where inter-user interference is negligible compared to noise [1]. ZF precoding nullifies IUI as well as the channel gain, performing well in scenarios where noise is weak compared to interference [2]. MMSE achieves a balance by maximizing a ratio between the signal gain at the intended user and the interference plus noise [3]. Nonlinear precoding stems from Dirty Paper Coding (DPC), which is capacityachieving for downlink MIMO channels [4]-[6]. However, its impractical complexity limits the application in reality. Alternatively, Tomlinson-Harashima Precoding (THP) offers a suboptimal solution with less complexity [7]. The performance

Table I: Conventional Precoding and Modulation methods

Waveform Design	Precoding			Modulation	
Methods	MMSE	DPC	THP	OFDM	OTFS
Linearity	Linear	Nonlinear		Linear	
CSI Requirement	Yes		No		
Cancellation Types	IUI		ISI	ISI-ICI	
Error Source	Imperfect CSI		ICI	IDI	

of precoding techniques is affected by the accuracy of CSI and nonlinear precoding methods are generally more sensitive to CSI errors than linear precoding methods [8].

Modulation techniques are widely investigated for interference cancellation in the time, frequency, and delay-Doppler domains by designing orthogonal data carriers. Orthogonal Frequency-Division Multiplexing (OFDM) modulation transmits symbols in the frequency domain to avoid interference in the time domain, known as Inter-Symbol Interference (ISI). However, when the channel experiences Doppler shift, OFDM suffers from interference in the frequency domain, known as Inter-Carrier Interference (ICI). Orthogonal Time-Frequency Space (OTFS) modulation [9] has been proposed to avoid both ISI and ICI by designing orthogonal data carriers in the delay-Doppler domain. However, in rapidly time-varying channels, there exists interference in the delay-Doppler domain, called Inter-Doppler Interference (IDI), which prevents OTFS symbols from maintaining orthogonality. Meanwhile, Fourier Transform (FT) based methods only design data carriers in the time, frequency, and delay-Doppler domains, which are unable to find jointly orthogonal bases when incorporating the space domain. Table I summarizes the conventional precoding and modulation methods. The waveform design based on these modulation and precoding methods treats interference separately, thereby failing to mitigate joint interference.

A joint spatio-temporal precoding method based on HOGMT [10] has been proposed to cancel joint interference in the spatio-temporal domain by projecting the transmitted signal onto the eigenspace of the spatio-temporal channels. Meanwhile, Multi-dimensional Eigenwave Multiplexing (MEM) modulation has been proven to cancel interference across all DoF with perfect CSI by decomposing high-dimensional channels into eigenwaves and using those as data carriers [11]. However, since both methods require eigen decomposition of the channel, their performance degrades with CSI errors, which is common in real-world scenarios. This motivates us to propose a joint interference cancellation method robust to the imperfect CSI. In this paper, we show that the convolution

operation of the CNN is equivalent to the wireless system. For a CNN with a single linear kernel, the kernel itself is exactly the same as the transmitted signal. Therefore, the objective of CNN training in our method is to obtain a desired kernel for one-time transmission rather than a general model. The contributions of this paper are summarized as follows:

- We show the equivalence between CNN and the wireless system, revealing that, with the CSI and the desired signal as inputs, the single linear kennel of CNN converges to the optimal transmitted signal in MMSE.
- The proposed method cancels spatial interference while avoiding post-coding steps, thereby reducing the computational burden at the receiver.
- The proposed method is adaptive to both perfect and imperfect CSI cases and can be extended to highdimensional channels for joint interference cancellation.
- We validate the accuracy and generality of the proposed method by extensive simulations in three cases: 1) Spatial channels with the perfect CSI, 2) Spatial channels with the imperfect CSI and 3) Spatio-temporal channels with imperfect CSI. The comparison with SoTA is provided.

II. PRELIMINARIES

A. Channel Representations and Domain Transformations

In Linear Time-Variant (LTV) channels, the transmitted signal s(t) is impacted by the underlying physics of the channel, described by path delays and Doppler shift to produce the received signal r(t) [12] as,

$$r(t) = \sum_{p=1}^{P} h_p s(t - \tau_p) e^{j2\pi\nu_p t}$$
 (1)

where h_p , τ_p and ν_p are the path attenuation factor, time delay and Doppler shift for path p, respectively. We omit the noise term for simplicity. Then (1) is expressed in terms of the overall delay τ and Doppler shift ν as

$$r(t) = \iint_{\Gamma} S_H(\nu, \tau) s(t - \tau) e^{j2\pi\nu t} d\tau d\nu$$
 (2)

$$= \int h(t,\tau)s(t-\tau) \ d\tau \tag{3}$$

where $S_H(\nu,\tau)$ is the (Doppler-delay) spreading function and $h(t,\tau)$ is the time-varying impulse response, which describes the channel gains for all paths in the Doppler-delay domain and the time-delay domain, respectively. The time-frequency and frequency-Doppler representation can be obtained by

$$L_H(t,f) = \iint S_H(\nu,\tau)e^{j2\pi(t\nu - f\tau)} d\tau d\nu \tag{4}$$

$$b(f,\nu) = \iint h(t,\tau)e^{j2\pi(-t\nu - f\tau)} dt d\tau$$
 (5)

where $L_H(t, f)$ and $b(f, \nu)$ are the TF transfer function and spectrum transfer function, respectively.

Since all the channels can be transformed to the time-delay domain, we use $h(t,\tau)$ to characterize the interference in the LTV channels without considering the space domain.

<u>Interpretation:</u> For Linear Time-Invariant (LTI) channels, $\overline{h(t,\tau)}$ and $\overline{S}_H(\nu,\tau)$ collapse to $h(\tau)$; $b(f,\nu)$ and $L_H(t,f)$ collapses to H(f). OFDM with cyclic prefix achieves close-optimal performance since there is no Doppler shift (ICI-free).

B. Joint Spatio-Temporal Precoding: HOGMT Precoding

For the spatio-temporal (time-varying MIMO) channels, $h(t,\tau)$ is extended to incorporate multiple users. For simplicity, we consider the single-antenna user case. Denotes $h_{u,u'}(t,\tau)$ [13] as the time-varying impulse response between the u'-th transmit antenna and the u-th user. The 4-D channel tensor is expressed by

$$\mathbf{H}(t,\tau) = \begin{bmatrix} h_{1,1}(t,\tau) & \cdots & h_{1,u'}(t,\tau) \\ \vdots & \ddots & \\ h_{u,1}(t,\tau) & & h_{u,u'}(t,\tau) \end{bmatrix}$$
(6)

HOGMT precoding [8] cancels the spatial, temporal and joint spatio-temporal interference existing in $\mathbf{H}(t,\tau)$. Let $k_{u,u'}(t,t')=h_{u,u'}(t,t-t')$ be the 4-D channel kernel [12], [14], (3) is rewritten as the spatio-temporal case

$$r(u,t) = \iint k(u,t;u',t')s(u',t') \ du' \ dt'$$
 (7)

By HOGMT, the 4-D channel kernel k(u,t;u',t') is decomposed into eigen components as follows,

$$k(u, t; u', t') = \sum_{n=1}^{N} \sigma_n \psi_n(u, t) \phi_n(u', t')$$
 (8)

with orthonormal properties as

$$\langle \psi_n(u,t), \psi_{n'}^*(u,t) \rangle = \delta_{nn'} \langle \phi_n(u,t), \phi_{n'}^*(u,t) \rangle = \delta_{nn'}$$
(9)

The two decomposed eigenfunction sets show duality as

$$\int k(u,t;u',t')\phi_n^*(u',t') \ du' \ dt' = \sigma_n \psi_n(u,t)$$
 (10)

The eigenfunctions with the above duality is known as *dual eigenfunctions*. (10) shows that transmitting a eigenfunction through the channel, its dual will be received at the receiver. Then the precoded signal x(u,t) based on HOGMT is derived by combining the jointly orthogonal eigenfunctions with the desired coefficients x_n as,

$$x(u,t) = \sum_{n=1}^{N} x_n \phi_n^*(u,t) \text{ where, } x_n = \frac{\langle s(u,t), \psi_n(u,t) \rangle}{\sigma_n}$$
 (11)

<u>Interpretation:</u> Since HOGMT precoding projects the entire signal onto the eigenspace spanned by eigenfunctions $\{\phi_n\}$ and $\{\psi_n\}$, its accuracy is influenced by two main aspects: 1) the number of eigenfunctions, which affects the completeness of the signal projection, and 2) the accuracy of the CSI, which affects the correctness of the decomposed eigenfunctions.

C. Multi-dimensional Modulation: MEM Modulation

MEM [11] employs eigenfunctions (also known as eigenwaves) as data carriers, multiplexing the data symbols $\{s_n\}$

and eigenfunctions $\{\phi_n\}$ as,

$$x(u,t) = \sum_{n=1}^{N} s_n \phi_n^*(u,t)$$
 (12)

Transmitting x(u,t) over the channel, the data carrier ϕ_n is converted to its dual ψ_n scaled by subchannel gains σ_n according to (10). Therefore, the received signal is given by

$$r(u,t) = \sum_{n=1}^{N} \sigma_n s_n \psi_n(u,t) + v(u,t)$$
 (13)

where v(u,t) is the AWGN. Since eigenfunctions are orthogonal, the estimate symbol $\{\hat{s}_n\}$ can be obtained by the demultiplexing using the conjugate of $\{\psi_n\}$ at the receiver as,

$$\hat{s}_n = \iint r(u, t) \psi_n^*(u, t) \ du \ dt = \sigma_n s_n + v_n \tag{14}$$

Interpretation: Unlike HOGMT precoding projecting the entire signal onto eigenfunctions, MEM transmits each symbol independently. Therefore, the number of eigenfunctions does not affect the accuracy but does affect the throughput. However, since it involves a demultiplexing step, i.e., matched filtering using eigenfunctions at the receiver, CSI is required at both the transmitter (CSIT) and the receiver (CSIR). Inconsistency between them will lead to demultiplexing errors.

III. LEARNING TO CANCEL JOINT INTERFERENCE

By the nature of wireless systems, the received signal is obtained by the convolution of the channel gains and the transmitted signal as shown in (3). Considering the work principle of the CNN is also based on convolution, it is promising to find a mapping between them. From a system view, the input, CNN kernel and the output correspond to the transmitted signal, the channel and the received signal, respectively. However, this mapping is meaningless as our objective is to optimize the transmitted signal. Noticing the interchangeability of the convolution variables, the input can serve as the channel while the CNN kernel acts as the transmitted signal. Meanwhile, since the signal is linear and there is no "multiple layers" of signals in reality, the CNN kernel must be one linear layer. Thus the interference cancellation is solved by Theorem 1.

Theorem 1. (JIC-CLK) Given imperfect CSI $\tilde{\mathbf{H}} = \mathbf{H} + \Delta \mathbf{H}$, where $\Delta \mathbf{H} \sim \mathcal{N}(0, \sigma_{\Delta \mathbf{H}})$ and modulated symbols \mathbf{s} , CNN with a single linear kernel \mathbf{w} minimizes the loss function in (15)

$$\mathcal{L} = \frac{1}{B} \sum_{b=1}^{B} ||\mathbf{w}(\tilde{\mathbf{H}}_b) - \mathbf{s}||^2$$
s.t. $||\mathbf{w}||^2 \le P$ (15)

such that employing the kernel \mathbf{w} as the transmitted signal minimizes the interference in MMSE sense. Where $\mathbf{w}(\cdot)$ is the kernel operation. $\tilde{\mathbf{H}}_b$ is one batch imperfect CSI and B is the batch size. P is the power constraint.

Proof. Transmitting a signal x through the channel \tilde{H} , the interference is expressed by $\tilde{H}x-s$. Then the optimal transmitted signal w with respect to interference cancellation in

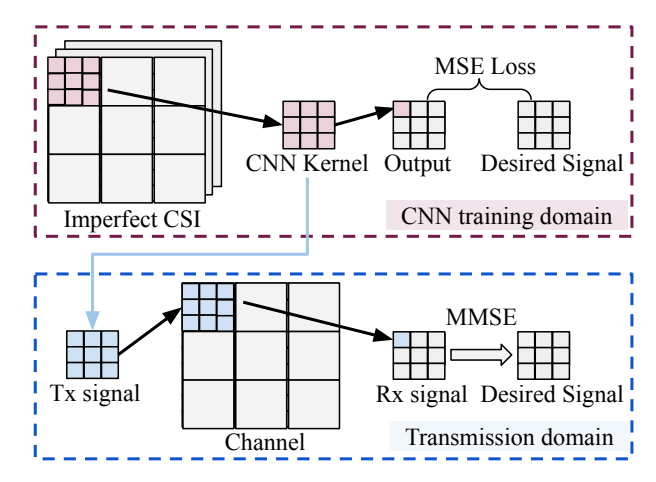


Figure 1: The connection between the training domain and the transmission domain for a 3x3 signal example.

MMSE is obtained by solving

$$\underset{\mathbf{x}}{\operatorname{arg\,min}} \quad \mathbb{E}\{||\tilde{\mathbf{H}}\mathbf{x} - \mathbf{s}||^2\}$$
s.t.
$$||\mathbf{x}||^2 \le P$$
(16)

For CNN with one linear kernel, we have $\mathbf{w}(\mathbf{H}) = \mathbf{H}\mathbf{w}$. Comparing (15) and (16), we observe that the kernel \mathbf{w} is equivalent to the transmitted signal \mathbf{x} . Therefore, CNN minimizing \mathcal{L} enables \mathbf{w} converging to the optimal \mathbf{x} with respect to minimal interference in MMSE.

Extension to high-dimensional channels: In the spatiotemporal channels, the imperfect CSI is represented by a 4-D tensor with added errors, $\tilde{\mathbf{H}}(t,\tau) = \mathbf{H}(t,\tau) + \Delta \mathbf{H}(t,\tau)$, where the entry is denoted as $\tilde{h}_{u,u'}(t,\tau)$, with u and u' as indices of antennas at the receiver and the transmitter, respectively. Let $\tilde{k}_{u,t}(u',t') = \tilde{h}_{u,u'}(t,t-t')$, \mathcal{L} is rewritten as

$$\mathcal{L} = \frac{1}{B} \sum_{h=1}^{B} ||\langle \tilde{k}_{u,t}(u',t'), w(u',t') \rangle - s(u,t)||^2$$
 (17)

where $\langle a,b\rangle$ is the inner product of a and b. w(u',t') and s(u,t) are 2-D forms of w and s in (15), respectively, which are spatio-temporal signals in the transmission domain.

Figure 1 shows the high-level view of JIC-CLK, where the inputs are the imperfect CSI and the desired signal. The linear CNN kernel is trained to minimize the MSE loss between the output and the desired signal, where the output is the received signal in the transmission domain. Therefore, transmitting the linear kernel over the channel renders the received signal to approach the desired signal in MMSE sense.

Remark 1. Since the received signal directly converges to the desired signal in MMSE, JIC-CLK eliminates the need for post-coding steps, thereby reducing the computational burden at the receiver. This is a crucial advantage for practical applications, especially for hardware-limited user equipment such as mobile phones and vehicular communication systems.

Remark 2. In general, conventional CNN methods are modeled as black boxes, where the kernels consist of multiple

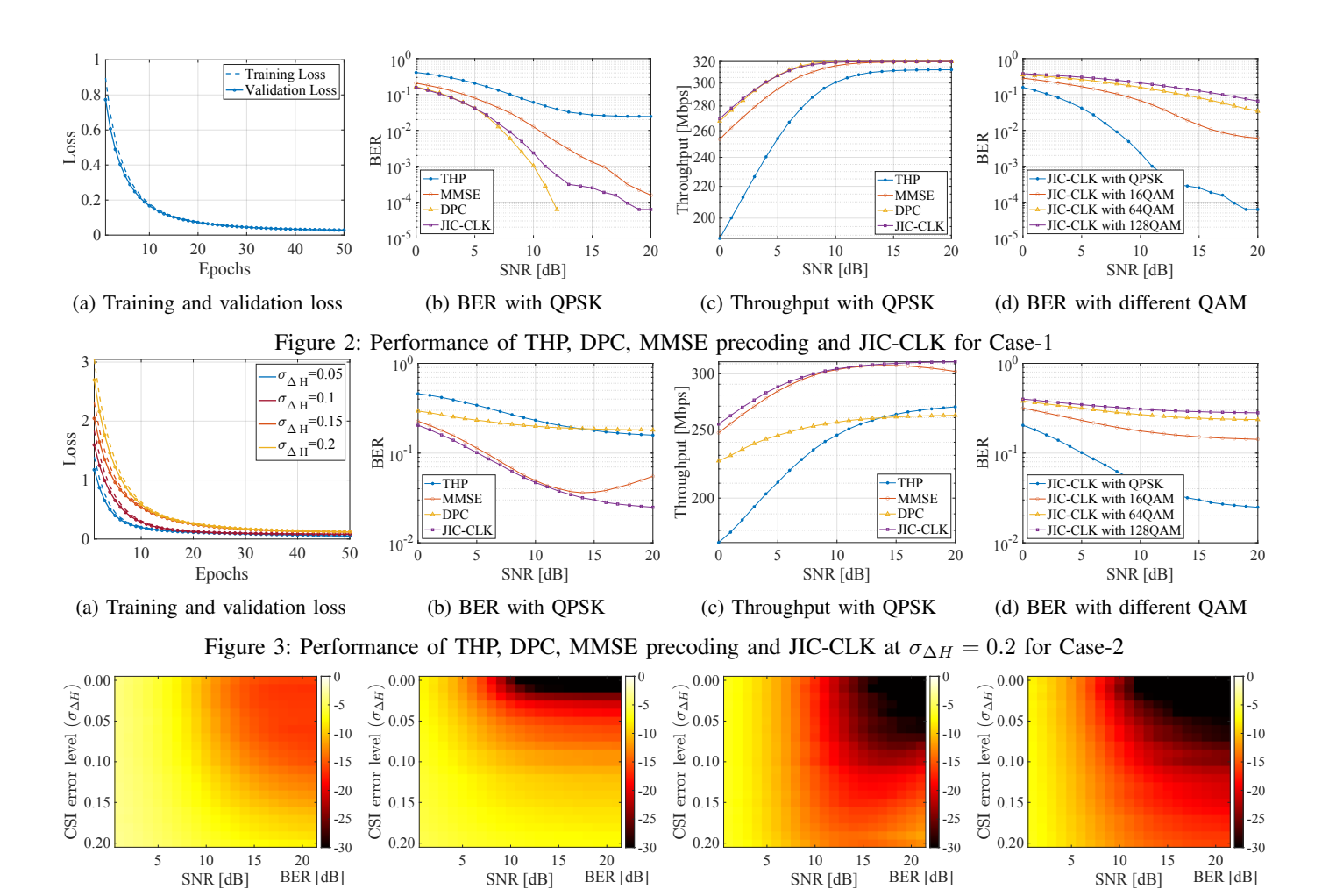


Figure 4: BER of THP, DPC, MMSE precoding and JIC-CLK over $\sigma_{\Delta H}$ for Case-2

(b) DPC

layers with nonlinear activation functions. Employing this type of CNN to optimize the transmitted signal, where the transmitted signal can only be the output of the CNN, cannot ensure convergence due to the following reasons: 1) the black box kernel lacks explainability, and 2) since both the CSI and data symbols are randomly generated, the trained model with a fixed kernel struggles to generalize to this double randomness.

IV. RESULTS

A. Case-1: Spatial Channels with Perfect CSI

(a) THP

In the training phase, we generate 1000 random channels $\mathbf{H} \in \mathbb{C}^{16 \times 16}$ with standard Gaussian distribution and data symbols $\mathbf{s} \in \mathbb{C}^{16 \times 1}$ pairs. For each pair, we conduct model training over 50 epochs, with each epoch consisting of 2000 identical samples (perfect CSI). The bandwidth is 20 MHz. During the testing phase, we obtain the transmitted signal $\mathbf{x} \in \mathbb{C}^{16 \times 1}$, which is the kernel, from the trained model and transmit it through the channel \mathbf{H} under an AWGN environment with varying Signal-to-Noise Ratio (SNR) conditions, ranging from 0 dB to 20 dB. The received signal $\mathbf{r} \in \mathbb{C}^{16 \times 1}$ is obtained by $\mathbf{r} = \mathbf{H}\mathbf{x} + \mathbf{v}$. We then compare the demodulated

r and s to compute the Bit Error Rate (BER).

(c) MMSE precoding

Figure 2a shows the training and validation loss, both of which converge within 50 epochs. Figure 2b compares the BER of THP, DPC, MMSE precoding and JIC-CLK with the QPSK scheme. JIC-CLK performs worse than DPC, which is reasonable since DPC is a capacity-achieving method with the perfect CSI. THP shows the highest BER as it is not suitable for large MIMO channels. JIC-CLK outperforms both MMSE and THP, achieving near-ideal BER from 0 dB SNR to around 5 dB SNR. Figure 2c shows that JIC-CLK achieves a similar throughput to DPC, and both outperform MMSE form 0 dB SNR to 10 dB SNR. THP has the lowest throughput. Figure 2d shows the BER of JIC-CLK with QPSK, 16QAM, 64QAM and 128QAM, where a higher-order QAM leads to a higher BER since more bits are modulated in one QAM symbol.

(d) JIC-CLK

B. Case-2: Spatial Channels with Imperfect CSI

With imperfect CSI, each sample is added an random error as $\tilde{\mathbf{H}} = \mathbf{H} + \Delta \mathbf{H}$ with $\Delta \mathbf{H} \sim \mathcal{N}(0, \sigma_{\Delta H}^2)$, where $\sigma_{\Delta H}$ represents the known CSI error variation. In this case, we set $\sigma_{\Delta H}$ from 0.01 to 0.2 with 0.01 steps. Other settings remain same as Case-1. Figure 3a shows the training and validation

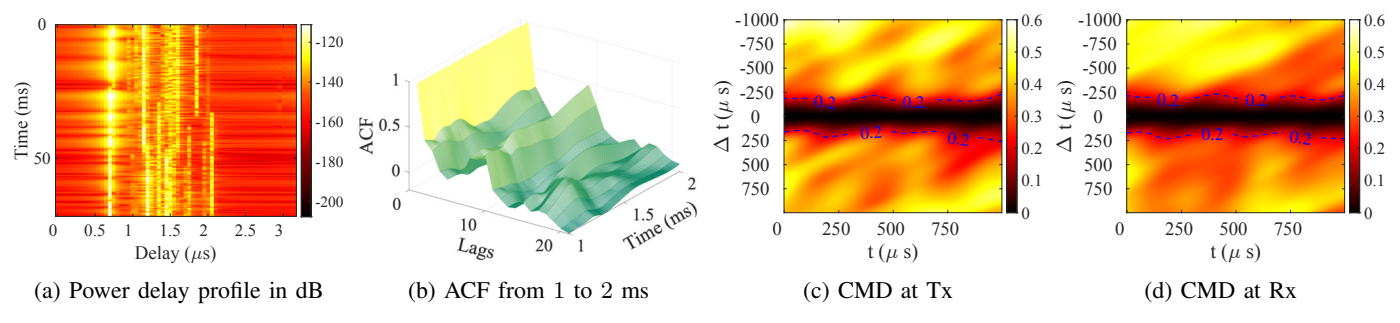


Figure 5: Channel profile and statistics in the time and space domain of Case-3

Table II: Parameters of the channel in Case-3

Parameter	Value		
Channel model	3GPP 38.901 UMa NLOS [15]		
Array type	BS: 3GPP 3-D [16]; UE: Vehicular [17]		
BS antenna	Height $h_b = 10$ m; Number $N_{u'} = 10$		
UE antenna	Height $h_u = 1.5$ m; User Number $N_u = 10$		
UE speed	$v \in [100, 150] \text{ km/h}$		
Bandwidth	Bw = 20 MHz; Center frequency: $f_c = 5$ GHz		
Channel size	Each segments: $\mathbf{H}(t,\tau) \in \mathbb{C}^{10 \times 10 \times 64 \times 64}$		

loss for $\sigma_{\Delta H} = 0.05, 0.1, 0.15$ and 0.2, respectively, where larger $\sigma_{\Delta H}$ leads to slower convergence. Figure 3b compares the BER at $\sigma_{\Delta H} = 0.2$. While DPC is optimal with perfect CSI, it is highly sensitive to CSI errors. MMSE precoding achieves a similar BER to JIC-CLK from 0 dB SNR to 10 dB SNR but degrades after 10 dB SNR. As the MMSE precoding matrix is $\mathbf{W}_{\mathbf{MMSE}} = \mathbf{H}^H (\mathbf{H}\mathbf{H}^H + \mathbf{I}/\mathbf{SNR})^{-1}$, the influence of the regularization term I/SNR diminishes as SNR increases, causing it to degrade to ZF precoding. This makes MMSE precoding more sensitive to CSI errors at high SNR levels. In this case, JIC-CLK achieves the lowest BER. The corresponding throughput is shown in Figure 3c, where TPC performs the worst before 13 dB SNR but better than DPC thereafter. JIC-CLK outperforms the other three methods. Figure 3d compares the BER of JIC-CLK with varying QAM schemes at $\sigma_{\Delta H}=0.2$, where All QAM schemes except QPSK perform poorly, with BER larger than 10^{-1} .

Figure 4a-4d show the change in BER over $\sigma_{\Delta H}$ for the four methods. Overall, THP has the highest BER, while DPC is the most sensitive to CSI errors. MMSE precoding shows some robustness in the low SNR region due to the regulazation term in the precoding matrix. As SNR increases, it becomes more sensitive to CSI errors despite experiencing less noise. In contrast, the robustness of JIC-CLK is not affected by SNR, which achieves the best performance with imperfect CSI.

C. Case-3: Spatio-temporal Channels with Imperfect CSI

The spatio-temporal channel is generated using 3GPP 38.901 UMa NLOS senario built on QuaDriga in Matlab. The channel parameters and the layout of the base station (BS) and the user equipment (UE) are shown in Table II. As THP, DPC and MMSE precoding are unavailable for spatio-temporal channels, we compare our method with HOGMT precoding and MEM modulation in Case-3. As discussed in

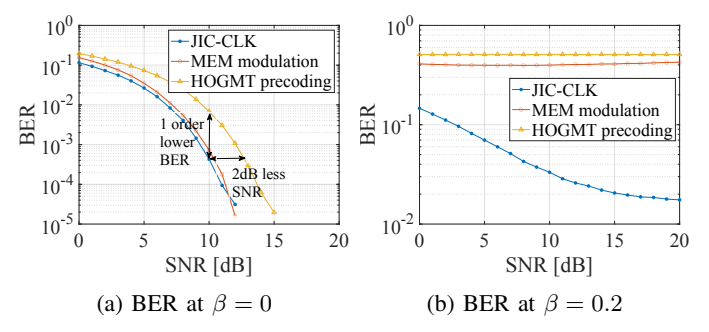


Figure 6: BER of HOGMT precoding, MEM modulation and JIC-CLK at $\beta = 0$ and $\beta = 0.2$, respectively.

the Section II, the number of eigenfunctions N have different effects on HOGMT precoding and MEM modulation. For a fair comparison, we choose the top 98% eigenfunctions for both methods. Since $\mathbf{H}(t,\tau)$ is not standard Gaussian distributed in Case-3, we set $\sigma_{\Delta H} = \beta \cdot \text{Var}(\mathbf{H}(t,\tau))$, where β is from 0 to 0.2 with 0.01 steps. It represents the relative CSI error variation. The number of samples is 18000. Figure 5a and 5b show the power delay profile and autocorrelation function (ACF) for the first user, respectively. A drift is observed due to the mobility of the user, leading to the time-varying distribution in overview. Correlation Matrix Distance (CMD) is a measure of the stationary interval in the space domain [18]. Figure 5c and 5d show the CMD at the transmitter and the receiver, respectively, where they are presented over time instead of distance because the varying mobility profiles of multiple users lead to different distances over time.

Figure 6a compares the BER of HOMGT precoding, MEM modulation and JIC-CLK at $\beta=0$, i.e., with perfect CSI. MEM modulation and JIC-CLK achieve a similar BER, both outperforming HOMGT precoding by around 1 order of magnitude at 10 dB SNR. They can achieve a similar BER as HOMGT precoding by using 2 dB less SNR. Figure 6b shows the BER of three methods at $\beta=0.2$, where JIC-CLK achieves a significantly lower BER than both HOGMT precoding and MEM modulation. Figure 7a-7c show the change of BER over β for three methods. There is a significant performance gap for HOGMT precoding between perfect CSI and imperfect CSI. As discussed in the "interpretation" in Section II-B, HOMGT precoding projects the entire signal onto the eigenfunctions. Consequently, any error in an eigenfunction will affect the reconstruction of the entire signal. In

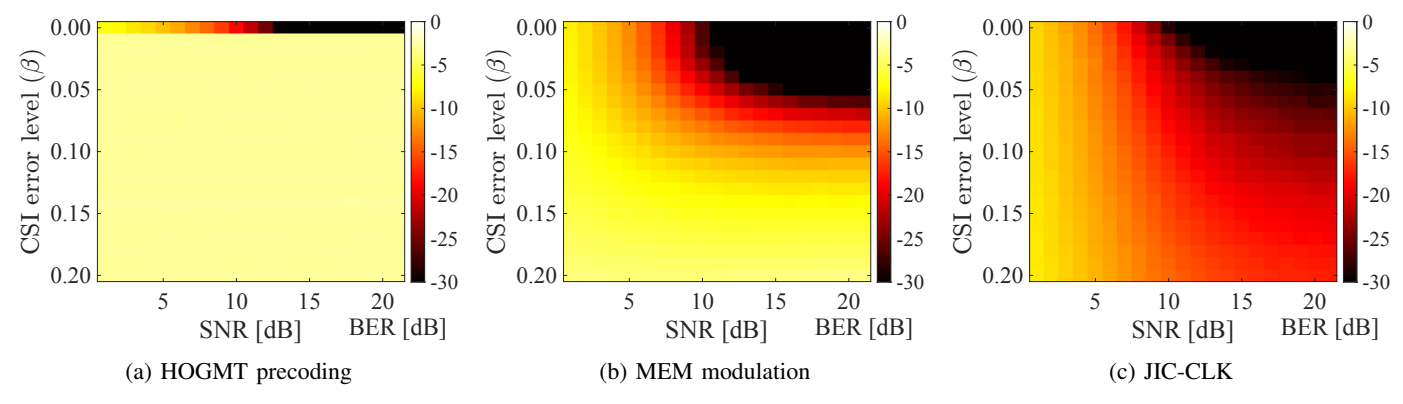


Figure 7: BER of HOGMT precoding, MEM modulation and JIC-CLK over β for Case-3

contrast, MEM modulation transmits symbols independently over each eigenfunction. Therefore, an error in an eigenfunction will only affect the symbol corresponding to that eigenfunction. MEM modulation shows a certain robustness at the low CSI error region, but degrades rapidly when $\beta>0.05,$ while JIC-CLK shows a slow and smooth degradation of BER over the entire CSI error region without abrupt jumps and significant fluctuations. This indicates a more predictable and consistent performance decline, showing that JIC-CLK is more robust to CSI errors compared to the other two methods.

V. DISCUSSION

Although the complexity is not the focus of this paper, it is important to note that employing the CNN kernel as the transmitted signal requires retraining for each transmission, while each transmission can include multiple data frames. Since JIC-CLK involves only one linear CNN kernel, the complexity remains practical, particularly in scenarios where the CSI error is large and the robustness is critical, such as underwater and High-speed train and V2X channels.

VI. CONCLUSION

In this paper, we proposed a joint interference cancellation method by leveraging the equivalence between the wireless system and a CNN with a single linear kernel. By transmitting the CNN kernel through the channel, the received signal approaches the desired signal in the MMSE sense without requiring post-coding steps. We demonstrate that for spatial channels with perfect CSI, JIC-CLK achieves near-ideal BER from 0 dB SNR to around 5 dB and outperforms both THP and MMSE precoding. With imperfect CSI, it surpasses THP, DPC, and MMSE precoding. For spatio-temporal channels with imperfect CSI, it is more robust than both HOGMT precoding and MEM modulation.

REFERENCES

- [1] T. Lo, "Maximum ratio transmission," *IEEE Transactions on Communications*, vol. 47, no. 10, pp. 1458–1461, 1999.
- [2] N. Jindal, "MIMO Broadcast Channels With Finite-Rate Feedback," IEEE Transactions on Information Theory, vol. 52, no. 11, pp. 5045– 5060, 2006.

- [3] Y. S. Cho, J. Kim, W. Y. Yang, and C. G. Kang, MIMO-OFDM Wireless Communications with MATLAB. Wiley Publishing, 2010.
- [4] S. Vishwanath, N. Jindal, and A. Goldsmith, "Duality, achievable rates, and sum-rate capacity of Gaussian MIMO broadcast channels," *IEEE Transactions on Information Theory*, vol. 49, no. 10, pp. 2658–2668, 2003
- [5] J. Lee and N. Jindal, "High SNR Analysis for MIMO Broadcast Channels: Dirty Paper Coding Versus Linear Precoding," *IEEE Transactions on Information Theory*, vol. 53, no. 12, pp. 4787–4792, 2007.
- [6] H. Weingarten, Y. Steinberg, and S. Shamai, "The Capacity Region of the Gaussian Multiple-Input Multiple-Output Broadcast Channel," *IEEE Transactions on Information Theory*, vol. 52, no. 9, pp. 3936–3964, 2006.
- M. Tomlinson, "New automatic equaliser employing modulo arithmetic," Electronics Letters, vol. 7, pp. 138–139(1), March 1971. [Online]. Available: https://digital-library.theiet.org/content/journals/10.1049/el_ 19710089
- [8] Z. Zou, M. Careem, A. Dutta, and N. Thawdar, "Unified Characterization and Precoding for Non-Stationary Channels," in ICC 2022 - IEEE International Conference on Communications, 2022, pp. 5140–5146.
- [9] R. Hadani, S. Rakib, M. Tsatsanis, A. Monk, A. J. Goldsmith, A. F. Molisch, and R. Calderbank, "Orthogonal time frequency space modulation," in 2017 IEEE Wireless Communications and Networking Conference (WCNC). IEEE, 2017, pp. 1–6.
- [10] Z. Zou, M. Careem, A. Dutta, and N. Thawdar, "Joint Spatio-Temporal Precoding for Practical Non-Stationary Wireless Channels," *IEEE Trans*actions on Communications, vol. 71, no. 4, pp. 2396–2409, 2023.
- [11] Z. Zou, I. Amarasekara, and A. Dutta, "Learning to Decompose Asymmetric Channel Kernels for Generalized Eigenwave Multiplexing," in IEEE INFOCOM 2024 IEEE Conference on Computer Communications, 2024, to appear.
- [12] F. Hlawatsch and G. Matz, Wireless Communications Over Rapidly Time-Varying Channels, 1st ed. USA: Academic Press, Inc., 2011.
- [13] P. Almers, E. Bonek, A. Burr, N. Czink, M. Debbah, V. Degliesposti, H. Hofstetter, P. Kyosti, D. Laurenson, G. Matz, A. F. Molisch, C. Oestges, and H. Ozcelik, Survey of channel and radio propagation models for wireless MIMO systems. EURASIP Journal on Wireless Communications and Net-working, 2007.
- [14] G. Matz, "On non-WSSUS wireless fading channels," *IEEE Transactions on Wireless Communications*, vol. 4, no. 5, pp. 2465–2478, 2005.
- [15] 3GPP TR 38.901 v16.1.0, "5G; Study on channel model for frequencies from 0.5 to 100 GHz," 3rd Generation Partnership Project (3GPP), Tech. Rep., 11 2020.
- [16] 3GPP TR 37.885 v15.1.0, "Technical specification group radio access network; study on evaluation methodology of new vehicle-to-everything v2x use cases for lte and nr," 3rd Generation Partnership Project (3GPP), Tech. Rep., 09.
- [17] 3GPP TR 36.873 v12.5.0, "Technical Specification Group Radio Access Network; Study on 3D channel model for LTE," 3rd Generation Partnership Project (3GPP), Tech. Rep., 06.
- [18] O. Renaudin, V.-M. Kolmonen, P. Vainikainen, and C. Oestges, "Non-Stationary Narrowband MIMO Inter-Vehicle Channel Characterization in the 5-GHz Band," *IEEE Transactions on Vehicular Technology*, vol. 59, no. 4, pp. 2007–2015, 2010.